Catalysis Letters Vol. 98, Nos. 1, October 2004 (© 2004)

Comparison of two preparation methods in the redox properties of Pd/CeO$_2$/Ta/Si model catalysts: spin coating versus sputter deposition

Do Heui Kim[1,2*] and Seong Ihl Woo[1]

[1]*Department of Chemical and Biomolecular Engineering, and Center for Ultramicrochemical Process Systems, Korea Advanced Institute Science and Technology (KAIST), 373-1 Kusong-dong, Yusong-gu, Taejon, 305-701 South Korea*
[2]*Present address: Chemistry and Physics Science Division, Pacific Northwest National Laboratory, 902 Battelle Blvd., Mail Stop: K8-93, Richland, WA 99352*

Received 3 May 2004; accepted 6 August 2004

Pd/CeO$_2$/Ta/Si model catalysts were prepared by spin coating and sputter deposition method, and characterized by means of AFM, SEM and *in situ* XPS, especially focusing on the redox properties of Ce and Pd elements. Compared with thin CeO$_2$ films (about 2.2 nm), the thicker ones (about 22 nm) maintained Ce^{4+} oxidation state even after treatment with H$_2$ up to 500 °C while the presence of Pd facilitated the reduction of ceria. The reduction of ceria brought about following that of PdO, which was explained by the spillover of hydride in Pd to CeO$_2$ originating from hydrogen adsorption on the Pd surface. Compared with the sputter deposition method, spin coating produced the smaller size of Pd particles, thus leading to formation of the stable PdO species against hydrogen. Based on these results, a schematic model of Pd/CeO$_2$/Ta/Si was suggested and it might be assumed that spin coating method provided with an environment similar to the conventional impregnation.

KEY WORDS: AFM; CeO$_2$; model catalyst; Pd; spin coating; sputter deposition; XPS.

1. Introduction

The catalytic chemistry of precious metals/ceria systems has been a subject of increasing interest in recent years. The main technological application of these materials is in the catalytic treatment of automobile exhaust emissions. Moreover, ceria itself and ceria with a lot of metals also show a significant activity in syngas reactions and hydrocarbon oxidation. Among the precious metals/ceria systems, the Pd/ceria is getting attention due to the exhibition of a variety of interesting catalytic behavior. They are two key materials of Pd-only three-way catalyst formulations, and their importance is likely to increase as a result of efforts to reduce expensive Rh compound in the conventional Pt/Rh one and to further improve hydrocarbon oxidation at low temperature [1]. Previous studies clearly show evidence for close interaction between Pd, CeO$_{2-x}$ and Al$_2$O$_3$ compounds [2]. In addition, in the area of C$_1$ chemistry, early studies indicated that this combination produced both methane and methanol from CO/H$_2$ mixtures at high pressures [3]. It has been shown that Pd/CeO$_2$ is highly selective to methanol during CO$_2$ hydrogenation at high pressures [4]. Palladium/ceria catalysts have also been shown to be both active and selective in water–gas shift reactions [5]. With the important catalytic applications described above, fundamental studies of the interactions between ceria and Pd metals, especially by means of model catalysts, have been reported.

Gorte *et al.* [6,7] showed that in the case of CO oxidation and water–gas shift reaction, a second rate process has been observed which gives significant rate enhancements over that found on either Pd or ceria individually resulting from the combination studies of TPD and steady-state reaction. They prepared the model catalysts by spray pyrolysis of aqueous solution of Ce(NO$_3$)$_2$ on an α-Al$_2$O$_3$(0001) single crystal, followed by vapor deposition of Pd. Only one method, metal evaporation, was applied.

Spin coating, which is a well-known technique for the deposition of polymeric photo resist layers on substrates [8], is suggested to be an effective way to deposit small metal-precursor particles such as Cu, Zn, Pt and Co on flat substrates [9–11]. Supported metal catalysts have been prepared by a conventional impregnation method, however, which is not applicable to flat model supports due to the absence of stabilizing capillary forces. This leads to supported particles which differ widely in size and are unevenly distributed over the support. The spin coating method, which squirts solution of precursor on a substrate spinning at high frequency, mimics the wet chemical preparation route in which a centrifugal force replaces the capillary force. The centrifugal force ejects most solution from the substrate and leaves only a thin liquid film of uniform thickness on the substrate. When the solvent evaporates from this film, the solute deposits homogenously onto the substrate, leading to the narrow particle distribution. By changing spin coating parameters, two important characteristics of model catalysts can be adjusted:the loading and the morphology of the

---

* To whom all correspondence should be addressed.
E-mail: do.kim@pnl.gov

1011-372X/04/1000–0023/0

catalyst particles [9–11]. Using such a flat model catalyst has advantages on the parallel use of other surface science tools. For example, according to the work by van van den Oetellar [12], the MSI (metal-support interaction) was verified by the Cu/SiO_2 model catalysts prepared by spin coating. In addition, Brookshier and Goodman [13] reported the control of CuO particle size on SiO_2 by using spin coating method. As the interaction between ceria and Pd is known to be one of the important factors to determine the catalytic activity, the comparison of each preparation methods will be appreciable. In this study, Pd/CeO_2 model catalysts, prepared by sputter deposition and spin coating methods, are characterized by using SEM, AFM and *in situ* XPS, especially focusing on changes in the redox behavior of Pd and Ce elements originating from the interaction between two elements.

2. Experimental

2.1. Preparation of model catalyst

Si(111) wafer (n-type) was used as a substrate. Tantalum thin films were deposited with a thickness of 100 nm by RF magnetron sputtering method at Samsung Electronics Company, designated as Ta/Si. The thickness was verified by SEM experiment. CeO_2 thin film was deposited on Ta/Si by RF magnetron sputtering at ambient temperature with a power of 30 mW, designated as CeO_2/Ta/Si. The target material (CeO_2: 99.99%) was purchased from Superconductive components Inc. (USA). During the deposition, Ar pressure was maintained at 5×10^{-3} Torr. The CeO_2/Ta/Si sample was analyzed without further treatments. For the preparation of sputtered Pd model catalysts, the metallic Pd was deposited at room temperature under Ar pressure of 5×10^{-3} Torr at 10 mW by sputtering the Pd target (99.9%; Toshima Co. Japan). For the spin coated Pd model catalysts, 0.1 ml solution of 0.01 M $Pd(NO_3)_2$ dissolved in de-ionized water was loaded on CeO_2/Ta/Si by micropipette, followed by the spin coating at 5000 rpm for 30 sec. After deposition or spin coating, they were calcined under O_2 flow at 500 °C for 1 h, designated as as-received sample.

2.2. Characterization of model catalysts

In situ XPS study was used to investigate the redox behavior of Pd and CeO_2 in the model catalysts. Mg Kα X-ray at 300 W (30 kV and 10 mA) was radiated to the sample in SPECS LHS-10 surface analyzer (Germany). The pass energy was 23.6 eV and its base pressure was maintained at 1×10^{-9} Torr by the turbo molecular pump (TMP). A signal from Ce 3d u‴ as a BE standard at 917.0 eV was used to correct for charging on the substrate. The subtraction of background (Shirley method) and curve fitting were performed with SPECTRA software from SPECS Co. The gas (20% H_2/He, Matheson) entered into the high pressure cell, was controlled by means of the mass flow controller (MFC) (Brooks Co., 5890E) and their flow rate was 20 cm^3/min. Therefore, following the treatment by hydrogen for 1 h, it is possible to introduce the sample to the analysis chamber without exposing it to the air. The reduction treatment was sequentially performed for the same sample from the room temperature to 500 °C. The temperature was controlled with the accuracy of ± 5 °C. The detailed system is depicted in Figure 1. Roughness of the surface was measured under ambient room conditions by using AFM (Autoprobe CP, PSI). SEM (XLSFEG, Philips) was used to measure the thickness of the sample.

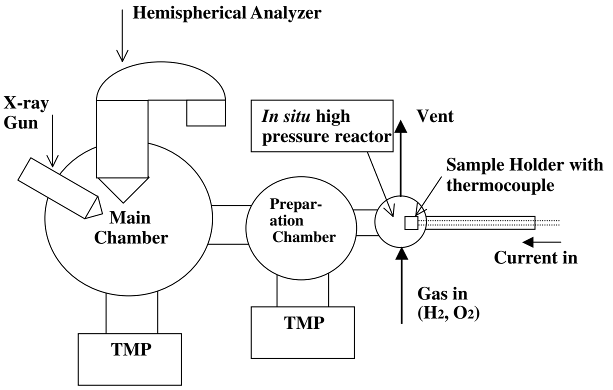

Figure 1. *In situ* XPS system. TMP is the abbreviation of turbo molecular pump.

3. Results and discussion

3.1. CeO_2/Ta/Si system

Figure 2 shows the Ce 3d photoelectron spectra as a function of deposition time. The exponential decay of the Ta 4f signal (not shown) as a function of CeO_2 deposition time clearly demonstrates the layer-by-layer growth rather than island-like growth. The complexity of the Ce 3d spectrum results from the final state effects of cerium. Based on the work of Creaser *et al.* [14], the spectrum can be assigned to four sets of doublets. The peaks labeled u are arising from $3d_{5/2}$ emissions, while the corresponding $3d_{3/2}$ emissions are labeled v. Peaks u‴ and v‴ have been assigned to primary photoemissions from Ce^{4+} cations, while the remaining three doublets correspond to different shakedown features [15]. As the deposition time increases, the fully oxidized Ce^{4+} features are shown. However, for less than 30 min of deposition, there are shoulders at 885.8 eV and 904.2 eV, representing peaks arising from Ce^{3+} [16]. It means that the mixture of CeO_2 and Ce_2O_3 exists together at the initial stage of deposition. Because the oxidation state of Ta was always maintained at 5+ for

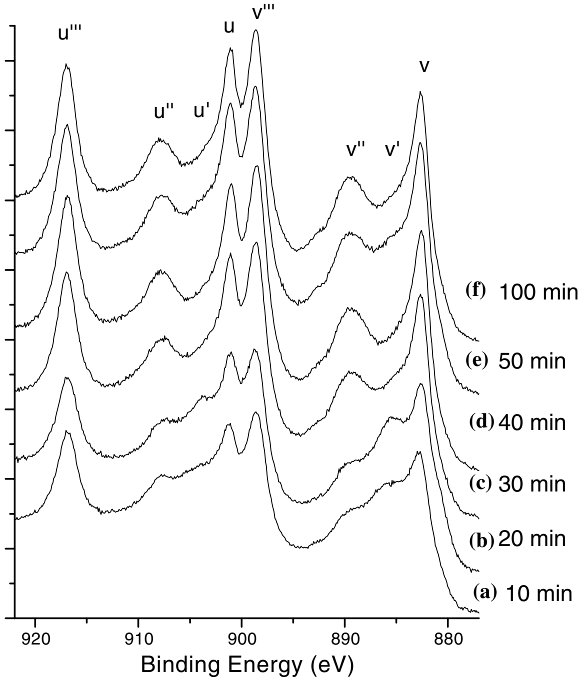

Figure 2. Ce 3d photoelectron spectra obtained for CeO_2 thin films sputter deposited on Ta/Si as a function of deposition time: (a) 10 min, (b) 20 min, (c) 30 min, (d) 40 min, (e) 50 min, (f) 100 min.

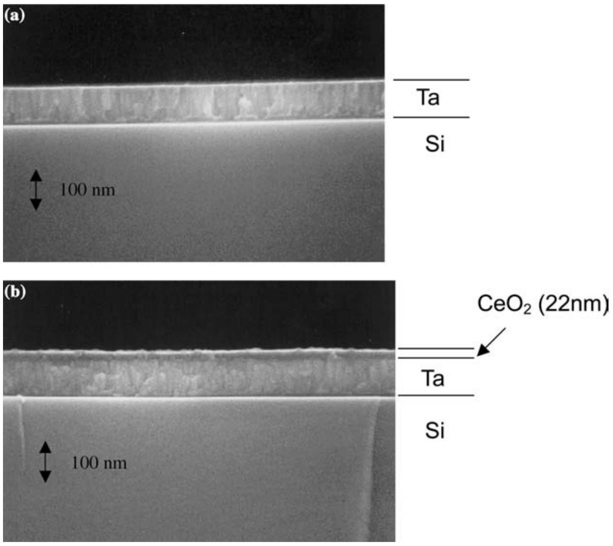

Figure 3. SEM cross-sectional pictures: (a) Ta/Si, (b) CeO_2 thin films sputter deposited for 100 min on Ta/Si. (×100,000).

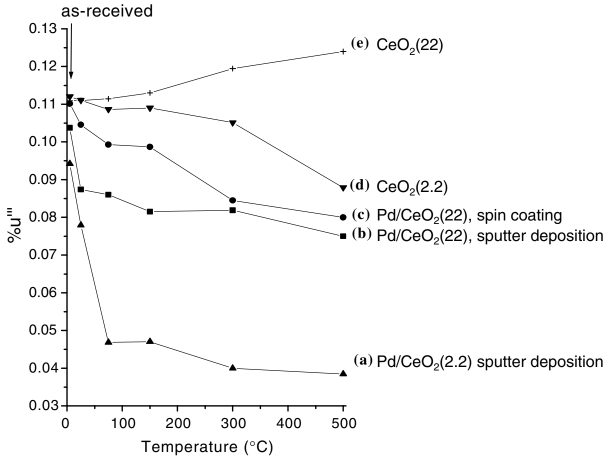

Figure 4. Change in %u‴ of Ce 3d during sequential reduction by H_2 with increasing temperatures:(a) sputter deposited Pd/CeO_2 (2.2 nm)/Ta/Si, (b) sputter deposited Pd/CeO_2 (22 nm)/Ta/Si, (c) spin coated Pd/CeO_2 (22 nm)/Ta/Si, (d) CeO_2 (2.2 nm)/Ta/Si, (e) CeO_2 (22 nm)/Ta/Si. All the CeO_2/Ta/Si samples were prepared by sputtering CeO_2 source on Ta/Si. The number in parenthesis indicates the thickness of CeO_2 films.

all the cases based on XPS results, we could exclude the possibility that CeO_2 was reduced by the reaction of Ta substrate. The disappearance of the shoulders is indicative of the formation of the fully oxidized ceria with Ce^{4+} cations only within the XPS detection limit. It is well corresponding to the work of Belton and Schieg [17]. They also observed the existence of Ce^{3+} in the thin CeO_2 film with the thickness of $\approx$0.6 nm and the formation of the fully oxidized CeO_2 film with the thickness of >5 nm. Figure 3 shows the SEM cross-sectional pictures of Ta/Si samples and the CeO_2 thin films deposited for 100 min on Ta/Si. It indicates that the thickness of CeO_2 is about 22 nm. Hereby, the sample CeO_2/Ta/Si after deposition for 100 min and for 10 min are denoted as CeO_2(22 nm)/Ta/Si and CeO_2(2.2 nm)/Ta/Si, respectively.

The u‴ peak in the Ce 3d spectrum has previously been used to assess the oxidation state of cerium [15]. For CeO_2, which contains only Ce^{4+}, the contribution of u‴ to the total area under the Ce 3d spectral envelope is 13–14%, and for the Ce_2O_3, which contains only Ce^{3+}, it approaches 0%. In the work of Shyu *et al.* [15], it was assumed that the relative magnitude of u‴ and the $Ce^{4+}/(Ce^{3+} + Ce^{4+})$ ratio are directly proportional, and the percent contribution of u‴ was used to assess the extent of Ce^{3+} formation. The effect of film thickness of CeO_2 on the redox behavior of CeO_2 is shown in figure 4, which is obtained from the integration of Ce 3d peak area. Both CeO_2(2.2 nm) and CeO_2(22 nm) show around 0.11 of %u‴, indicating the formation of Ce^{4+} after calcination. Reduction treatment above 300 °C makes CeO_2(2.2 nm)/Ta/Si decrease in %u‴ gradually, ascribed to the process that CeO_2 was partially reduced to Ce_2O_3. However, CeO_2(22 nm)/Ta/Si can keep the oxidation state as Ce^{4+} even after reduction at 500 °C. AFM surface images of CeO_2 (2.2 nm) and CeO_2 (22 nm) films are shown in figure 5 and figure 6, respectively. Although the roughness of thicker CeO_2(22 nm) films (figure 6) increases a little after calcinations (0.42 nm → 0.56 nm), that of thinner CeO_2(2.2 nm) films (figure 5) becomes much rougher (0.47 nm → 0.96 nm). The results of AFM and XPS lead to the summary that as CeO_2 thin

(a) as-deposited; rms roughness: 0.47 nm

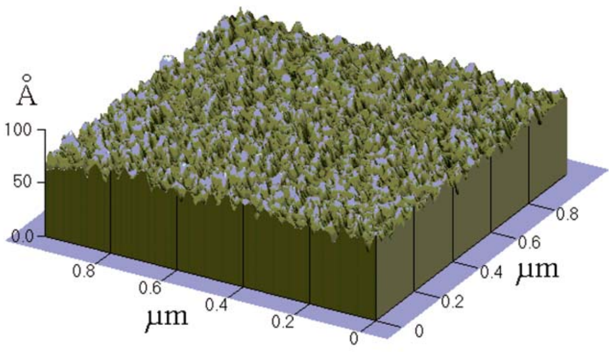

(b) calcined; rms roughness: 0.96 nm

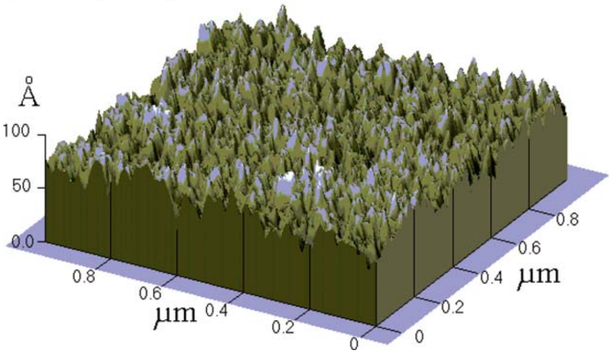

Figure 5. AFM surface images of CeO$_2$(2.2 nm)/Ta/Si samples: (a) as-received, (b) after oxidation at 500 °C for 1 h.

(a) as-deposited; rms roughness: 0.42 nm

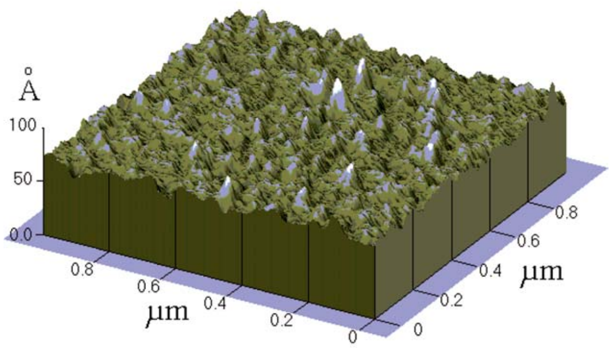

(b) calcined; rms roughness: 0.58 nm

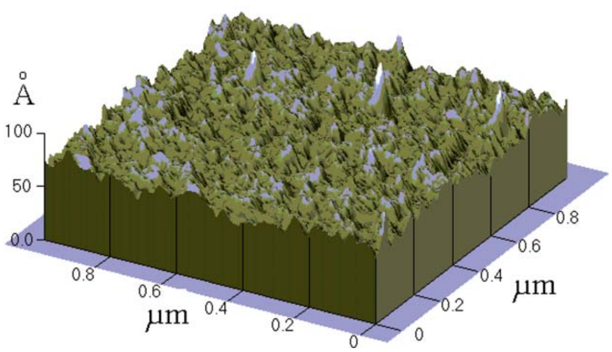

Figure 6. AFM surface images of CeO$_2$(22 nm)/Ta/Si samples: (a) as-received, (b) after oxidation at 500 °C for 1 h.

(a) spin coated Pd/CeO$_2$(22nm)

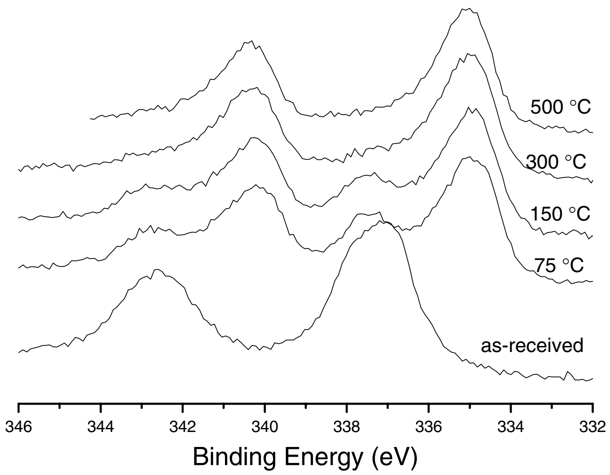

(b) sputter deposited Pd/CeO$_2$(22nm)

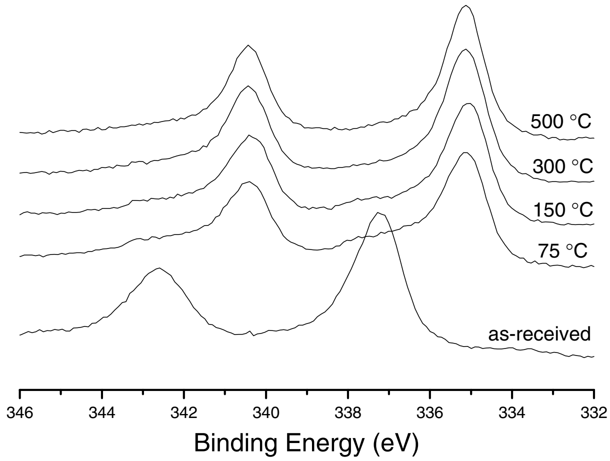

Figure 7. Pd 3d photoelectron spectra for (a) spin coated Pd/CeO$_2$(22 nm)/Ta/Si and (b) sputter deposited Pd/CeO$_2$(22 nm)/Ta/Si as a function of reduction temperature during sequential reduction with H$_2$.

films get thicker, they are harder to be reduced by H$_2$ and more stable upon oxidation at 500 °C. This is in good agreement with the previous result of Belton and Schimieg [17]. They compare the behavior of thick (> 5 nm) ceria layers to that of thin (0.4–0.8 nm) ceria islands. Under the reduction experiment, the thin ceria is reduced under UHV conditions whereas the thick ceria layers require high pressures (8 Torr) of CO in order to be reduced.

3.2. *Pd/CeO$_2$/Ta/Si system*

Figure 7 shows the change in Pd 3d spectra of sputter deposited and spin coated Pd/CeO$_2$/Ta/Si model catalysts. After the oxidation of the sample at 500 °C for 1 h, both samples show the binding energy of Pd 3d$_{5/2}$ around 337.0–337.5 eV, which is assigned to the formation of PdO. As the reduction temperature increases, a new peak around 335 eV brings about for both samples at the expense of the peak at 337.2 eV, indicating the vivid transformation from PdO to Pd. However, there is a clear difference in the transition temperature where the PdO is changed to Pd. In the sputter deposited sample, the metallic Pd is formed thoroughly after reduction with hydrogen at 75 °C. However, in the case of spin coated Pd/CeO_2/Ta/Si, the small peak arising from PdO still exists after reduction with H_2 at 150 °C and it disappears completely after reduction at 300 °C. It means that the Pd species in spin coated model catalysts requires higher reduction temperature. According to the same *in situ* XPS experiments with the sequential reduction for the Pd/Al_2O_3 heterogeneous catalysts [18], the smaller PdO particles, as evidenced by TEM and H_2 chemisorption, were reduced fully to the metallic state at 300 °C, while the bigger ones got reduced at room temperature. In addition, AFM data in figure 8 manifestly show the less roughness of the spin coated Pd/CeO_2/Ta/Si catalysts indicating the formation of the smaller particle size of Pd on CeO_2. By combining our results, it can be summarized that the Pd/CeO_2/Ta/Si model catalyst prepared by spin coating contains the smaller particle size of Pd, which requires higher reduction temperature than that by sputter deposition.

In comparison with two sputter deposited Pd/CeO_2/Ta/Si model catalysts with different thickness of CeO_2 (2.2 nm versus 22 nm), they show the similar trend in terms of the reducibility of PdO (not shown). It may suggest that the redox property of Pd species formed from sputter deposition is independent of the condition of CeO_2 support. On the other hand, the redox property of CeO_2 depends upon the particle size and thickness of Pd layer as shown in figure 4. The reduction to Ce^{3+} is greatly facilitated even following the reduction at 75 °C for Pd/CeO_2(2.2 nm)/Ta/Si model catalysts. In other words, Pd catalyzes the process of cerium reduction more severely on the thinner film of CeO_2. Compared with sputter deposited Pd/CeO_2(22 nm)/Ta/Si (figure 4b), the reduction of CeO_2 in the spin-coated one (figure 4c) is retarded at the temperature below 300 °C. Taking the reduction behavior of Pd 3d (figure 7) into consideration, it leads to the summary that the reduction of PdO is followed by that of CeO_2, ascribed to the process that hydrogen is migrating through the Pd metal layer to the CeO_2 layer.

(a) sputter deposited Pd/CeO_2(22nm); Rms roughness: 1.69 nm

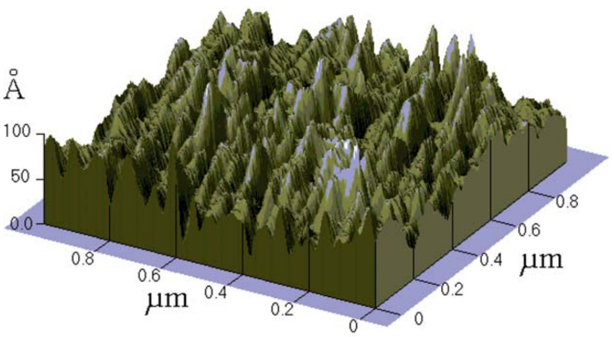

(b) spin coated Pd/CeO_2(22nm); Rms roughness: 0.94 nm

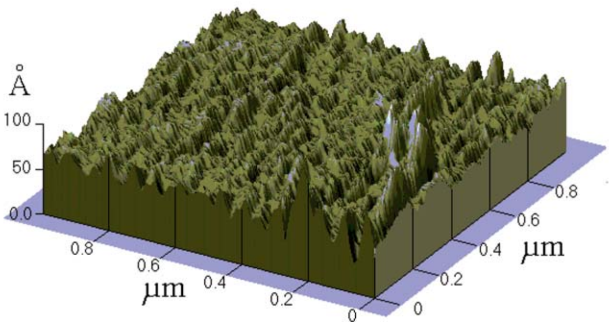

Figure 8. AFM surface images of (a) sputter deposited Pd/CeO_2(22 nm)/Ta/Si and (b) spin coated Pd/CeO_2(22 nm)/Ta/Si after calcination at 500 °C for 1 h.

3.3. Suggested model

It was shown that the redox behavior of CeO_2 was dependent on the thickness of the films and the presence of Pd. As the thickness decreases, the more easily reducible CeO_2 is formed because it is easier for the hydrogen atoms to migrate through the thinner films, in good agreement with the previous results. In addition, Pd catalyzes the reduction of CeO_2 from the result of the change in $\%u'''$ compared with Pd-free CeO_2 (figure 4). This phenomenon can be accounted for by the role of Pd which initially reacts with hydrogen to form hydride. It was reported that the H atoms are very mobile and have the unique property of diffusion into the interior of palladium to readily form hydrides [19,20]. The hydrides on Pd are suggested to react with CeO_2, leading to the ceria reduction. It is very similar to the case of ceria on Rh(111) where intimate contact with Rh can enhance the ceria reduction via reaction with CO which initially adsorbs on Rh [17].

The reduction behavior of PdO is very noticeable since two different methods result in the rather different trends. The spin coated Pd/CeO_2/Ta/Si system contains PdO species which are hard to be reduced, compared with the sputter deposited one. AFM surface images demonstrate the formation of much rougher surface for the sputtered Pd/CeO_2/Ta/Si grown in this study, which implies the formation of Pd particles with larger diameter. From the results of the heterogeneous Pd catalysts [18], the size of Pd cluster affects the redox behavior of Pd. Compared with sputter deposition, spin coating provides the model catalyst with smaller Pd size. However, it is too dangerous to make a general conclusion that sputter deposition method always results in the larger particle size because the size and the number density of the particles are determined by a lot of nucleation conditions such as deposition rate, substrate temperature, number of defect sites on the

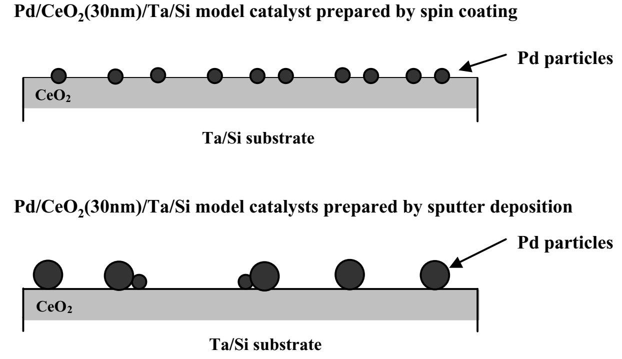

Figure 9. Schematic illustration of Pd/CeO$_2$/Ta/Si model catalysts prepared by spin coating and sputter deposition.

support, etc. [21]. Moreover, preparation of very smaller Pd clusters at 90 K was reported previously, whereas only comparatively large Pd particles were obtained at room temperature [22]. Although our limited condition (sputter deposition of Pd at room temperature) to prepare the model catalyst by using the sputter deposition prevents us from the generalization, the results clearly demonstrate that spin coating can be used as one of the promising methods to prepare the model catalyst which is able to provide with an environment that is similar to the "real catalyst system", or, "model catalyst". Based on our results, the schematic models of Pd/CeO$_2$/Ta/Si model catalysts prepared by spin coating and sputtering are illustrated in figure 9.

4. Conclusion

Pd/CeO$_2$/Ta/Si model catalysts were prepared by spin coating and sputtering method, and characterized by using AFM, SEM and *in situ* XPS. The thicker CeO$_2$ films (about 22 nm) showed the stable Ce^{4+} oxidation state after the reduction with H$_2$ up to 500 °C, although Pd made it possible for CeO$_2$ to be reduced under the same atmosphere at much lower temperature. The reduction of PdO proceeded that of ceria, attributed to the hydrogen adsorption on the Pd surface followed by the migration of hydrogen through the Pd layer to the ceria surface. Compared with sputtering method, spin coating method produced the smaller size of Pd as evidenced by AFM and *in situ* XPS. Based on these results, a schematic model of Pd/CeO$_2$/Ta/Si was suggested that spin coating provides this system with redox properties that is comparable to the conventional impregnation method.

Acknowledgment

This research was funded by the Center for Ultramicrochemical Process Systems sponsored by KOSEF. The author (DHK) expresses sincere thanks to Mr. Myoung Rae Kim and Dr. Samina Azad for the assistance of the experiment and the valuable discussion and comments, respectively.

References

[1] B.J. Cooper, Plat. Metals Rev. 38 (1994) 2.
[2] J.Z. Shyu, K. Otto, W.L.H. Watkins, G.W. Graham, R.K. Belitz and H.S. Gandhi, J. Catal. 114 (1988) 23.
[3] C. Sudhakar and M.A. Vannice, J. Catal. 95 (1985) 227.
[4] L. Fan and K. Fujimoto, Appl. Catal. 106 (1993) L1.
[5] S. Zhao, T. Luo and R.J. Gorte, J. Catal. 221 (2004) 413.
[6] T. Bunluesin, R.J. Gorte and G.W. Graham, Appl. Catal. B 14 (1997) 105.
[7] T. Bunluesin, R.J. Gorte and G.W. Graham, Appl. Catal. B 15 (1998) 107.
[8] W.W. Flack, D.S. Soong, A.T. Bell and D.W. Hess, J. Appl. Phys. 56 (1984) 1199.
[9] E.M. Kuipers, C. Laszlo and W. Wieldraaijer, Catal. Lett. 17 (1993) 71.
[10] R.M. van Hardeveld, P.L.J. Gunter, L.J. van Ijzendoorn, W. Wieldraaijer, E.W. Kuipersa and J.W. Niemantsverdriet, Appl. Surf. Sci. 84 (1995) 339.
[11] C. Doornkamp, C. Laszlo, W. Wieldraaijer and E.W. Kuipers, J. Mater. Res. 10 (1995) 411.
[12] L.C.A. van den Oetelaar, A. Partridge, S.L.G. Toussaint, C.F.L. Flipsea and H.H. Brongersma, J. Phys. Chem. B 102 (1998) 9541.
[13] M.A. Brookshier, C.C. Chusuei and D.W. Goodman, Langmuir 15 (1999) 2043.
[14] D.A. Creaser, P.G. Harrison, M.A. Morris and B.A. Wolfindale, Catal. Lett. 23 (1994) 13.
[15] J.Z. Shyu, W.H. Weber and H.S. Gandhi, J. Phys. Chem. 92 (1988) 4964.
[16] M. Alexandrou and R.M. Nix, Surf. Sci. 321 (1994) 47.
[17] D.N. Belton and S.J. Schmieg, J. Vac. Sci. Tech. A 11 (1993) 2330.
[18] D.H. Kim, S.I. Woo and O.-B. Yang, Appl. Catal. B 26 (2000) 285.
[19] R.J. Behm, V. Penka, M.-G. Cattania, K. Christmann and G. Ertl, J. Chem. Phys. 78 (1983) 7486.
[20] M.-G. Cattania, V. Penka, R.J. Behm, K. Christmann and G. Ertl, Surf. Sci. 126 (1983) 382.
[21] B. Kasemo, S. Johansson, H. Persson, P. Thormählen and V.P. Zhdanov, Topic. Catal. 13 (2000) 43.
[22] M. Bäumer and H.-J. Freund, Prog. Surf. Sci. 61 (1999) 127.